Supplementary Information

In silico screening and binding characterization of small molecules towards G-quadruplex structure formed in the promoter region of *c-MYC* oncogene

Jyotsna Bhat[¥a], Soma Mondal[¥a], Pallabi Sengupta[a], Subhrangsu Chatterjee[a*]

[a] Department of Biophysics, Bose Institute, P-1/12 CIT Scheme VIIM, Kankurgachi, Kolkata, WB, India.
[*]**Email:** subhro_c@jcbose.ac.in . [¥] These authors have contributed equally

Table of Contents

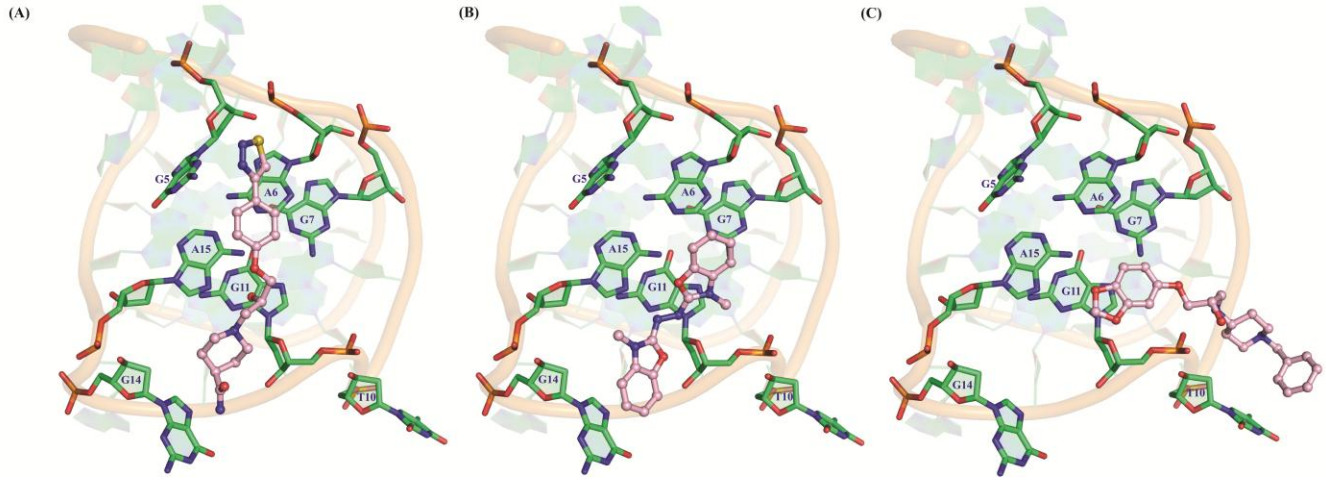

Figure S1: Binding conformation of ligands at 5' end of Pu27, (A) docked pose of TPP, (B) docked pose of RJC, (C) docked pose of AWO.

Table S1. *ADME properties predicted by QikProp and Docking Score selected molecules after virtual screening

SN. No	S	MW	QPlogPo/w	Q PlogS	Q PPCaco	Q PlogBB	PHOA	RO5	Glide Dock Score
Chelerythrine (CHE)	2	349.385	4.591	-4.969	9514.447	0.426	100	0	-5.259
TPP	0	362.446	0.548	-2.062	24.929	-1.219	55.151	0	-7.022
RJC	1	296.328	4.023	-4.787	5272.44	0.104	100	0	-7.698
AWO	0	384.474	2.632	-1.984	208.022	0.316	83.845	0	-7.040

SN No.= Supernatural drug database ID

S (STARS) = Number of property/descriptor values falling outside the 95% range of similar values for known drugs. Recommended value 0-5.

MW = Molecular weight

QPlogPo/w = Predicted octanol / water partition coefficient. Recommended values –2.0 – 6.5.

QPlogS = Predicted aqueous solubility, log S. Recommended values –6.5 – 0.5.

QPPCaco = Predicted apparent Caco-2 cell permeability in nm/sec. Recommended values <25 poor, >500 great.

QPlogBB = Predicted brain/blood partition coefficient. Recommended values –3.0 – 1.2.

PHOA= Predicted human oral absorption on 0 to 100% scale.Recommended values >80% is high <25% is poor

RO5= Rule of Five,The rules are: mol_MW < 500, QPlogPo/w < 5, donorHB ≤ 5, and accptHB ≤ 10.

* The scores given are approximate values as predicted by the software and not measured experimentally.

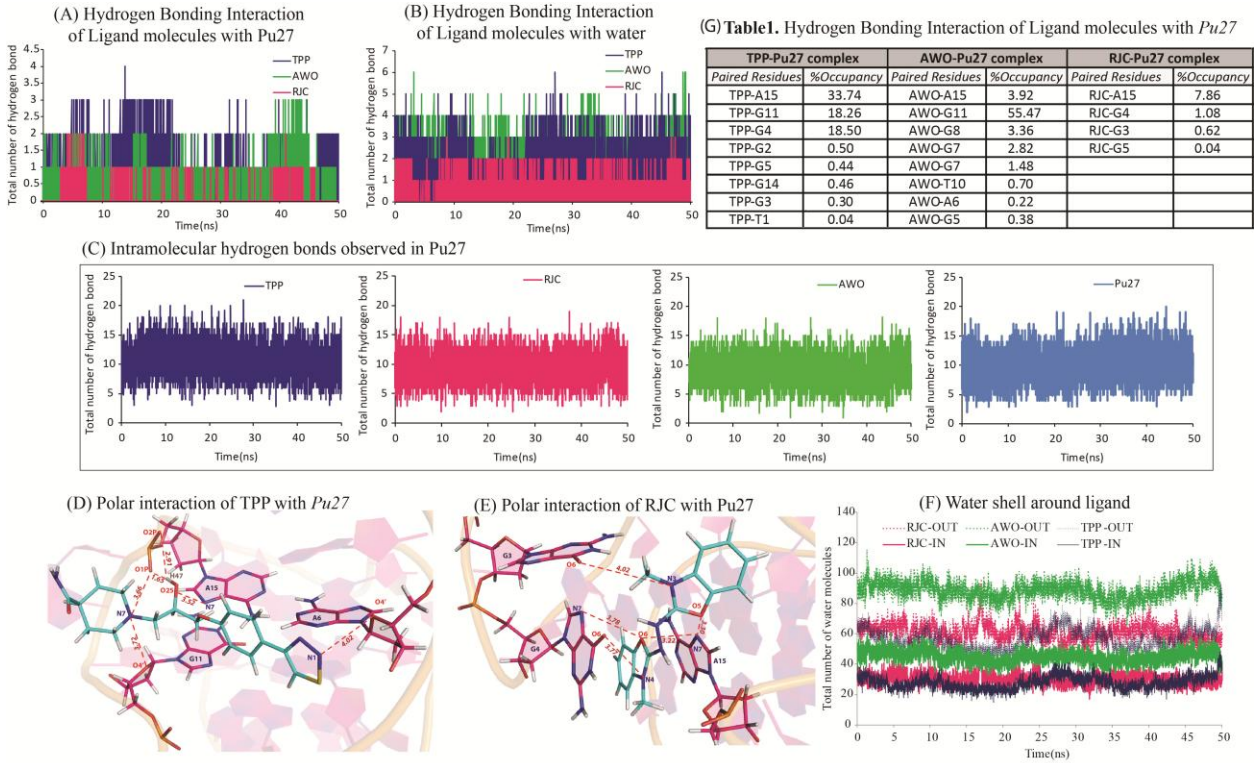

(G) **Table1.** Hydrogen Bonding Interaction of Ligand molecules with *Pu27*

TPP-Pu27 complex		AWO-Pu27 complex		RJC-Pu27 complex	
Paired Residues	*%Occupancy*	*Paired Residues*	*%Occupancy*	*Paired Residues*	*%Occupancy*
TPP-A15	33.74	AWO-A15	3.92	RJC-A15	7.86
TPP-G11	18.26	AWO-G11	55.47	RJC-G4	1.08
TPP-G4	18.50	AWO-G8	3.36	RJC-G3	0.62
TPP-G2	0.50	AWO-G7	2.82	RJC-G5	0.04
TPP-G5	0.44	AWO-G7	1.48		
TPP-G14	0.46	AWO-T10	0.70		
TPP-G3	0.30	AWO-A6	0.22		
TPP-T1	0.04	AWO-G5	0.38		

Figure S2: Hydrogen bond analysis [color key: unbound-*Pu27* (sky blue), *Pu27*-TPP complex (dark blue), *Pu27*-RJC complex (pink), *Pu27*-AWO complex (green)], (A) hydrogen bonding interactions among ligand molecules and *Pu27*, (B) hydrogen bonding interactions among ligand molecules and surrounding water molecules, (C) intra-molecular hydrogen bonding interactions in quadruplex region, (D) polar interactions between TPP and nucleotide bases sustained in last 1ns simulation period, (E) polar interactions between RJC and nucleotide bases sustained in last 1ns simulation period, (F) water shell analysis around respective ligand, (G) **Table 1**, enlisting occupancy of pair-wise hydrogen bonding interactions in Pu27-ligand complex systems.

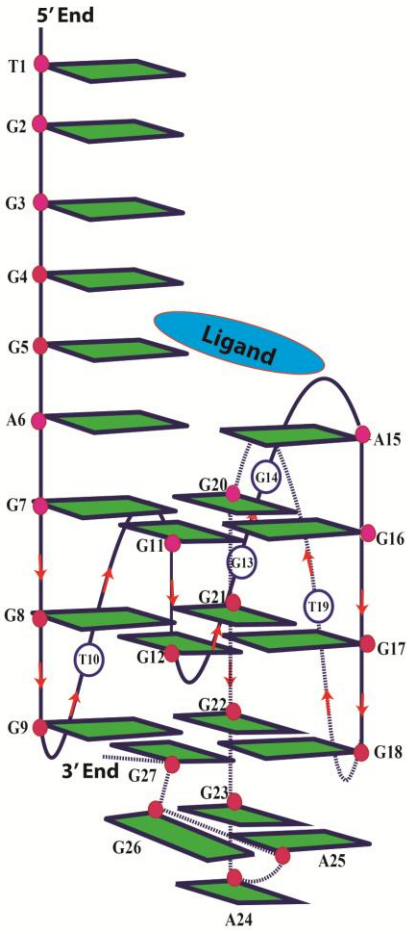

Table S2. Intra-molecular hydrogen bond interactions of Pu27 in various binding conditions

Paired Residue	TPP-Pu27complex	AWO-Pu27complex	RJC-Pu27complex	Pu27
T1-G8	0.00	0.00	3.24	0.00
G2-G3	31.5	0.02	0.82	0.02
G2-G4	16.86	0.00	0.66	0.02
G2-G5	0.00	0.00	6.42	0.00
G3-G4	0.00	0.00	0.00	25.68
G3-G5	0.00	0.04	7.20	0.00
G4-A15	54.98	0.02	0.02	0.40
A6-A15	69.02	20.26	23.54	69.14
G7-G20	71.14	30.89	70.91	76.42
G7-G11	52.04	67.71	63.77	62.12
G11-G16	68.06	64.43	70.11	67.44
G16-G20	73.58	66.67	70.77	64.78
G8-G12	54.02	37.83	55.37	41.7
G8-G21	55.58	34.23	57.11	52.14
G12-G17	51.82	36.93	45.15	49.56
G17-G21	46.2	27.71	55.05	47.5
G9-G22	67.08	64.61	67.03	67.82

1 5′ end Overhang 2 A-A mismatch 3 First G-stack 4 Second G-stack 5 Third G-stack

Figure S3: Schematic representation of topological arrangement of *Pu27* and Table S2, enlists occupancy of pair-wise intra-molecular hydrogen bonding interactions in quadruplex region.

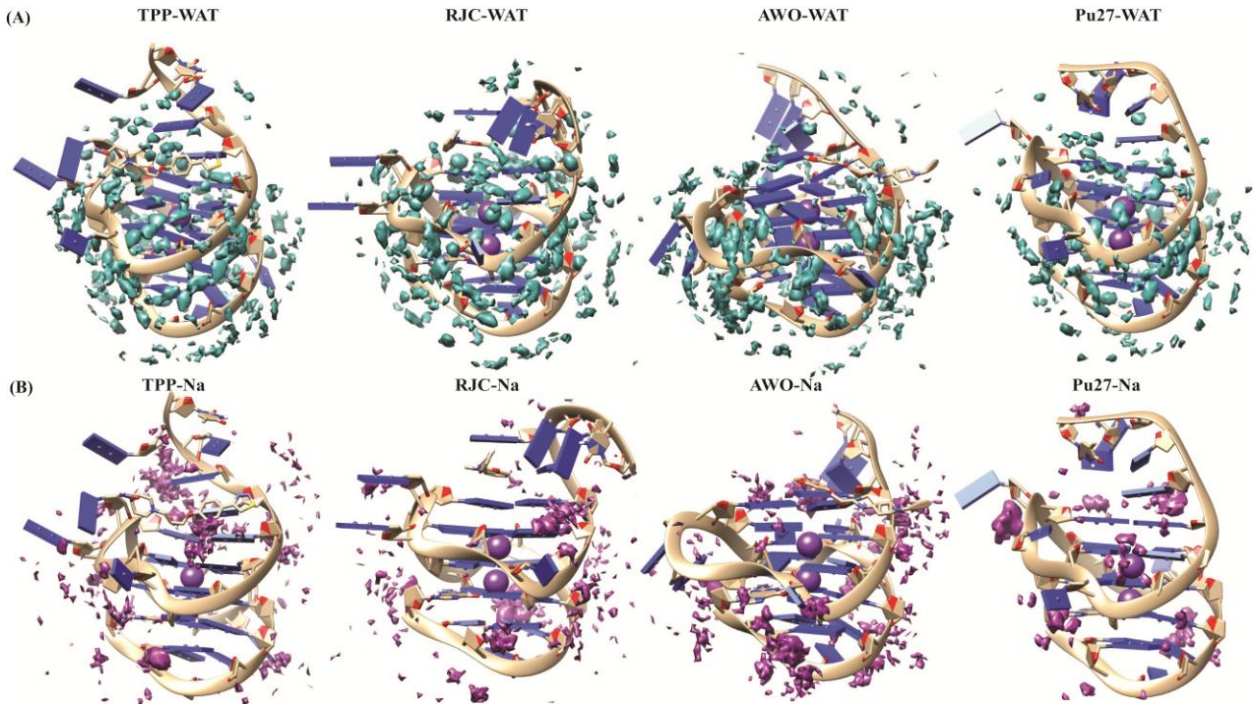

Figure S4: (A) Water grid density map of *Pu27* in different complexation states, (B) Ion grid density map of *Pu27* in different complexation states.

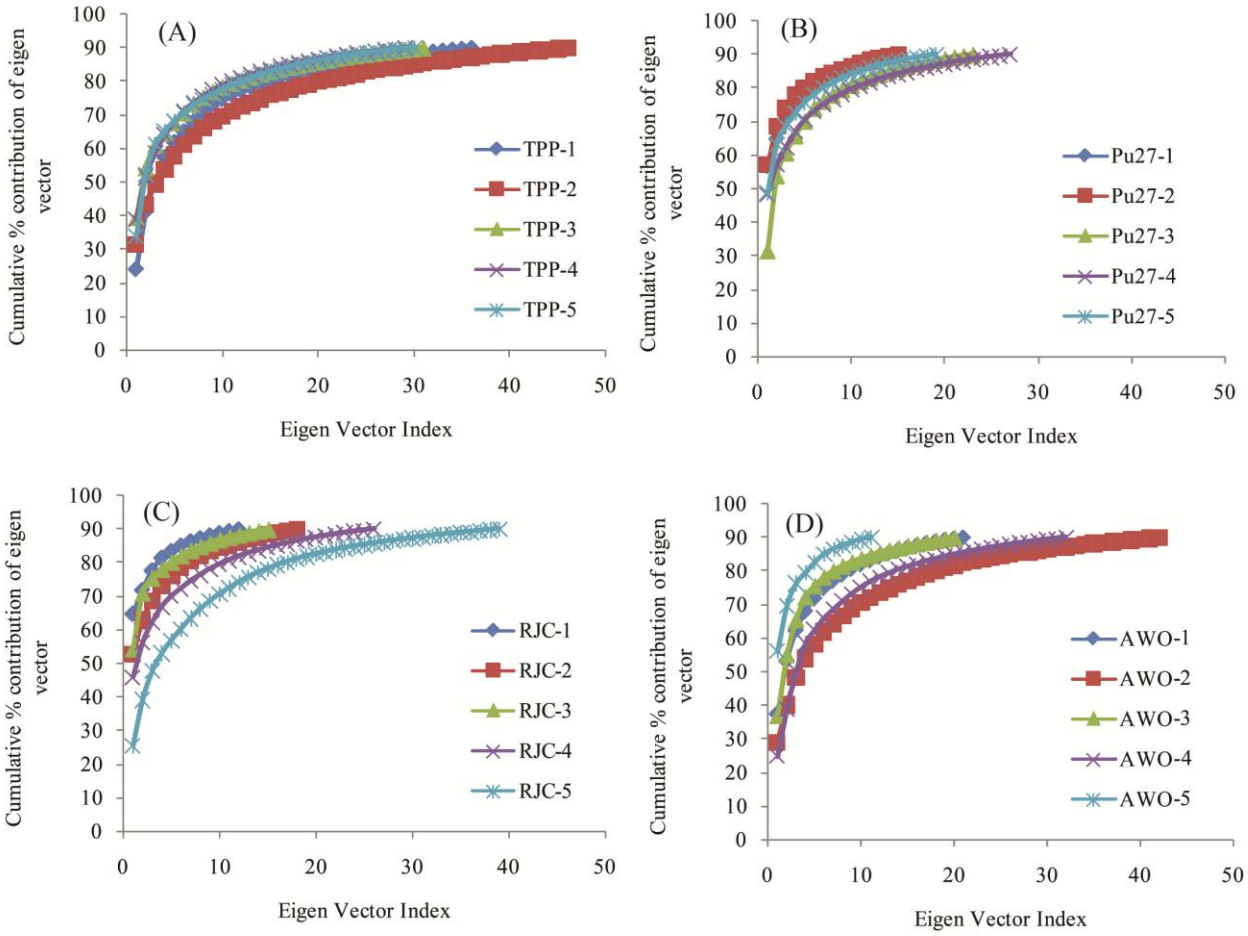

Figure S5: 'Cumulative % contribution of each eigenvector' for each trajectory derived from PCA analysis of (A) *Pu27*-TPP complex (B) unbound-*Pu27*, (C) *Pu27*-RJC complex and, (D) *Pu27*-AWO complex. 1: 0–10 ns, 2: 11–20 ns, 3: 21–30 ns, 4: 31–40 ns, 5: 41–50 ns time frames of each system are plotted.

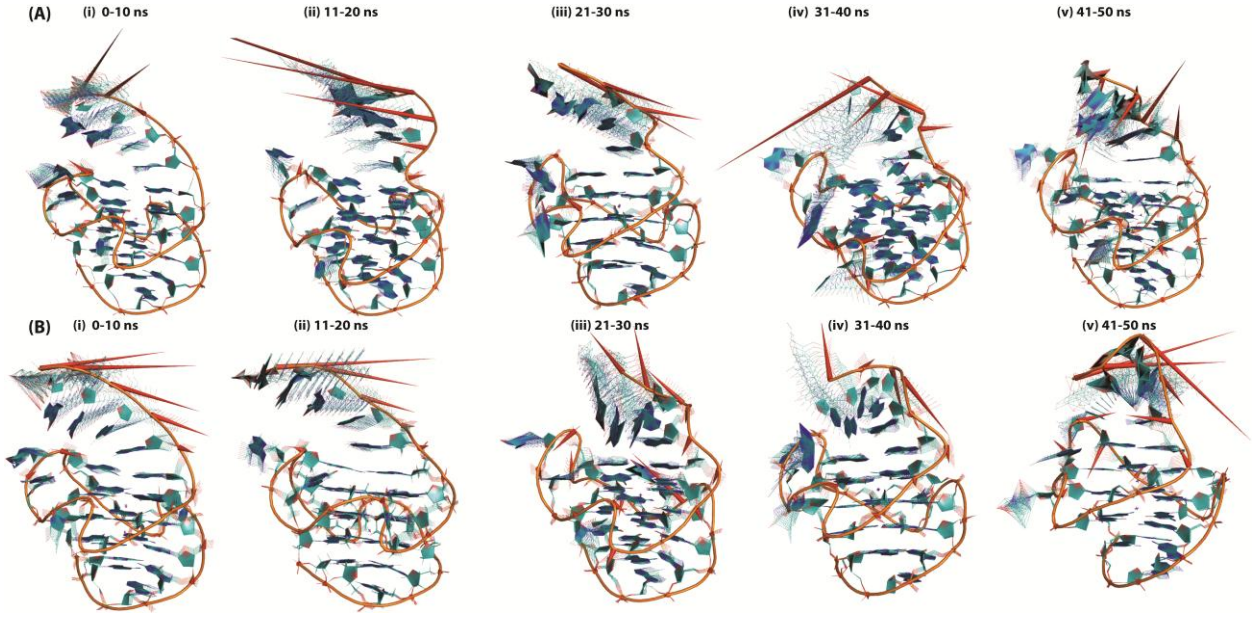

Figure S6: Porcupine plots of first (A) and second eigenvectors (B) of unbound-*Pu27*. Time frames are mentioned for respective plots. Blue color is for quadruplex structure (images are prepared in PyMOL).

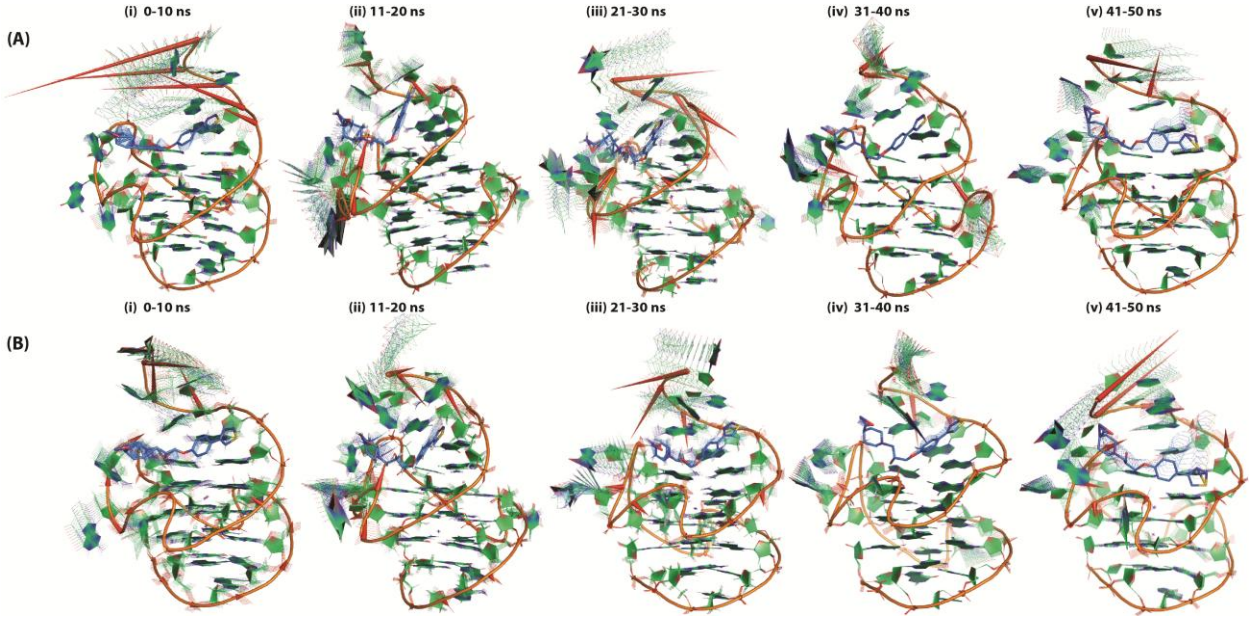

Figure S7: Porcupine plots of first (A) and second eigenvectors (B) of *Pu27*-TPP complex. Time frames are mentioned for respective plots. Green color is for quadruplex structure and blue color is for TPP molecule (images are prepared in PyMOL).

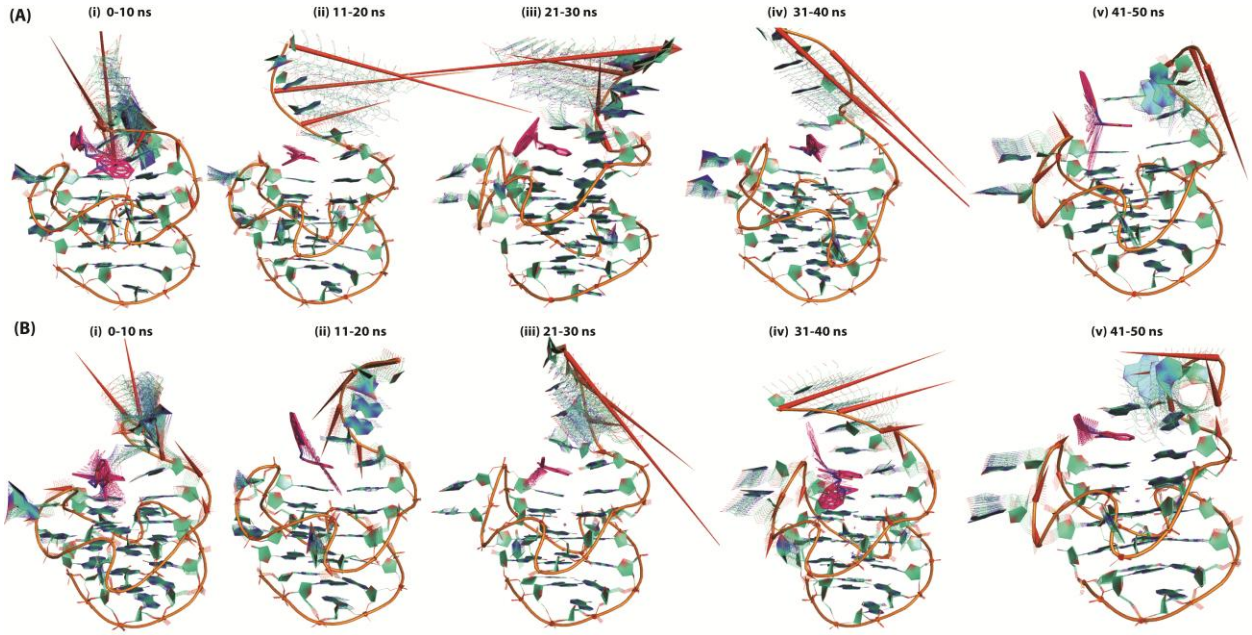

Figure S8: Porcupine plots of first (A) and second eigenvectors (B) of Pu27-RJC complex. Time frames are mentioned for respective plots. Green color is for quadruplex structure and magenta color is for RJC molecule (images are prepared in PyMOL).

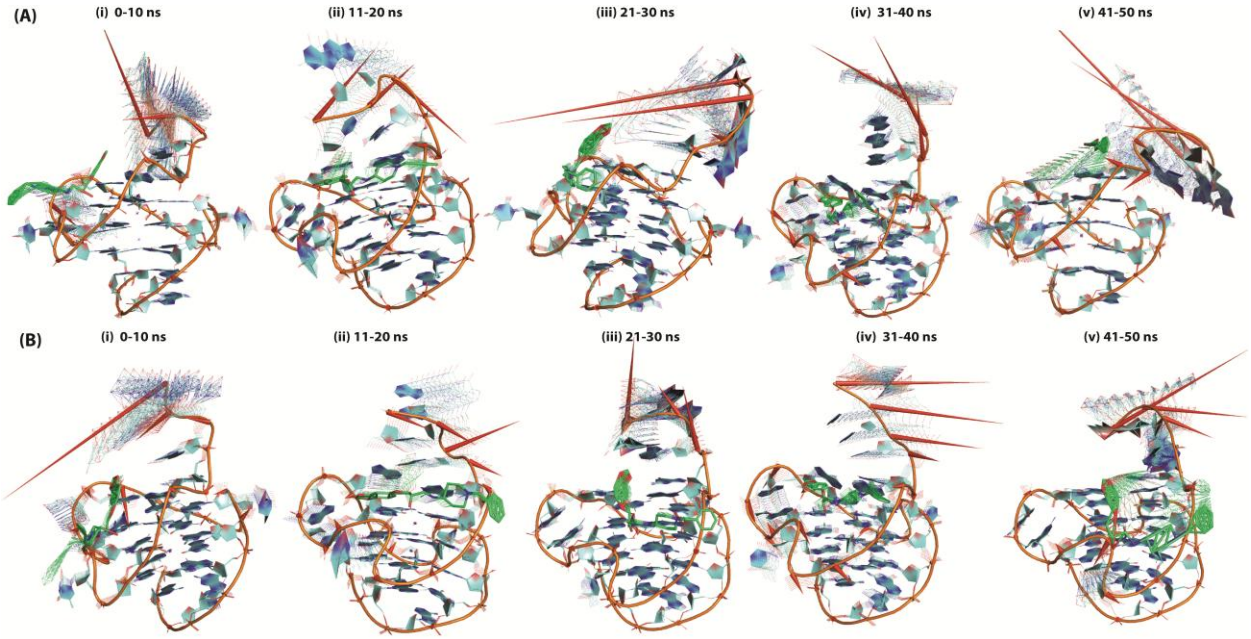

Figure S9: Porcupine plots of first (A) and second eigenvectors (B) of Pu27-AWO complex. Time frames are mentioned for respective plots. Blue color is for quadruplex structure and green color is for AWO molecule (images are prepared in PyMOL).

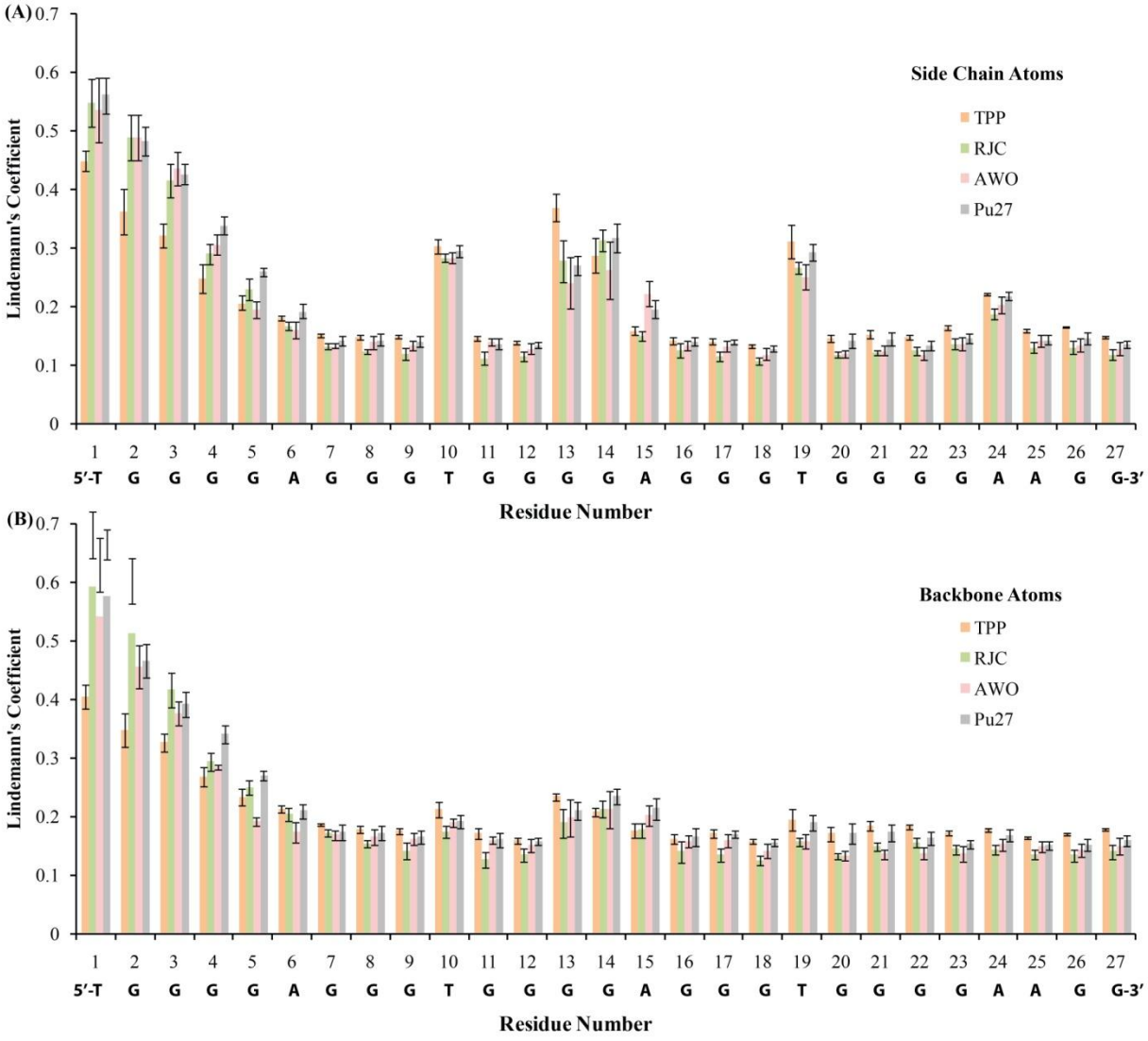

Figure S10: Lindemann's coefficient per residues is determined for clustered trajectories of *unbound*-Pu27, *Pu27*-TPP complex, *Pu27*-RJC complex and *Pu27*-AWO complex. Coefficients are calculated for all the five trajectories separately and average is plotted along with the standard error bars. Value < 0.15 indicates solid nature of residue whereas value > 0.15 indicates liquid nature. (A) Lindemann's coefficient calculated for side chain atoms of each residue, (B) Lindemann's coefficient calculated for backbone atoms of each residue.

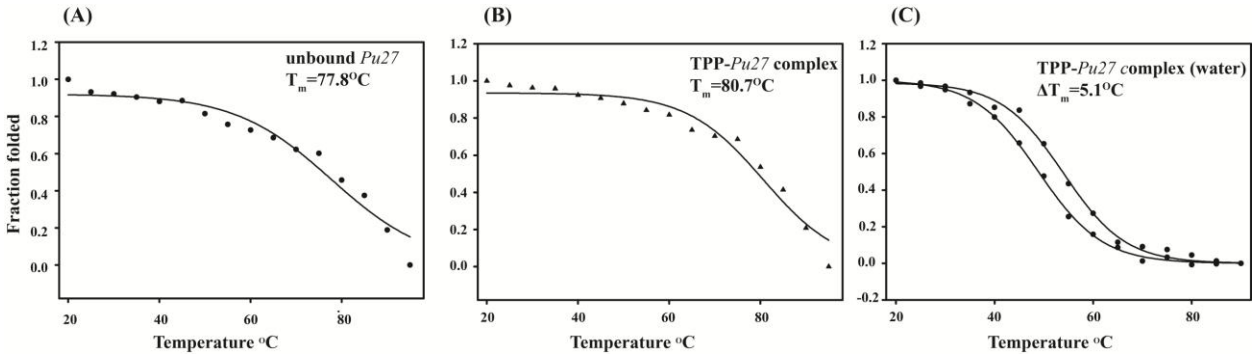

Figure S11: CD Melting experiments of *Pu27* and *Pu27*-TPP complex (A) Melting of unbound-*Pu27* 20µM in 10 mM Phosphate buffer, containing 100 mM KCl, pH 7.0. (B) Melting of *Pu27*-TPP complex (1:3) in 10 mM Phosphate buffer, containing 100 mM KCl, pH 7.0.(C) Melting of unbound-*Pu27* and *Pu27*-TPP complex, when the samples were annealed in water containing KCl < 1.5 mM.

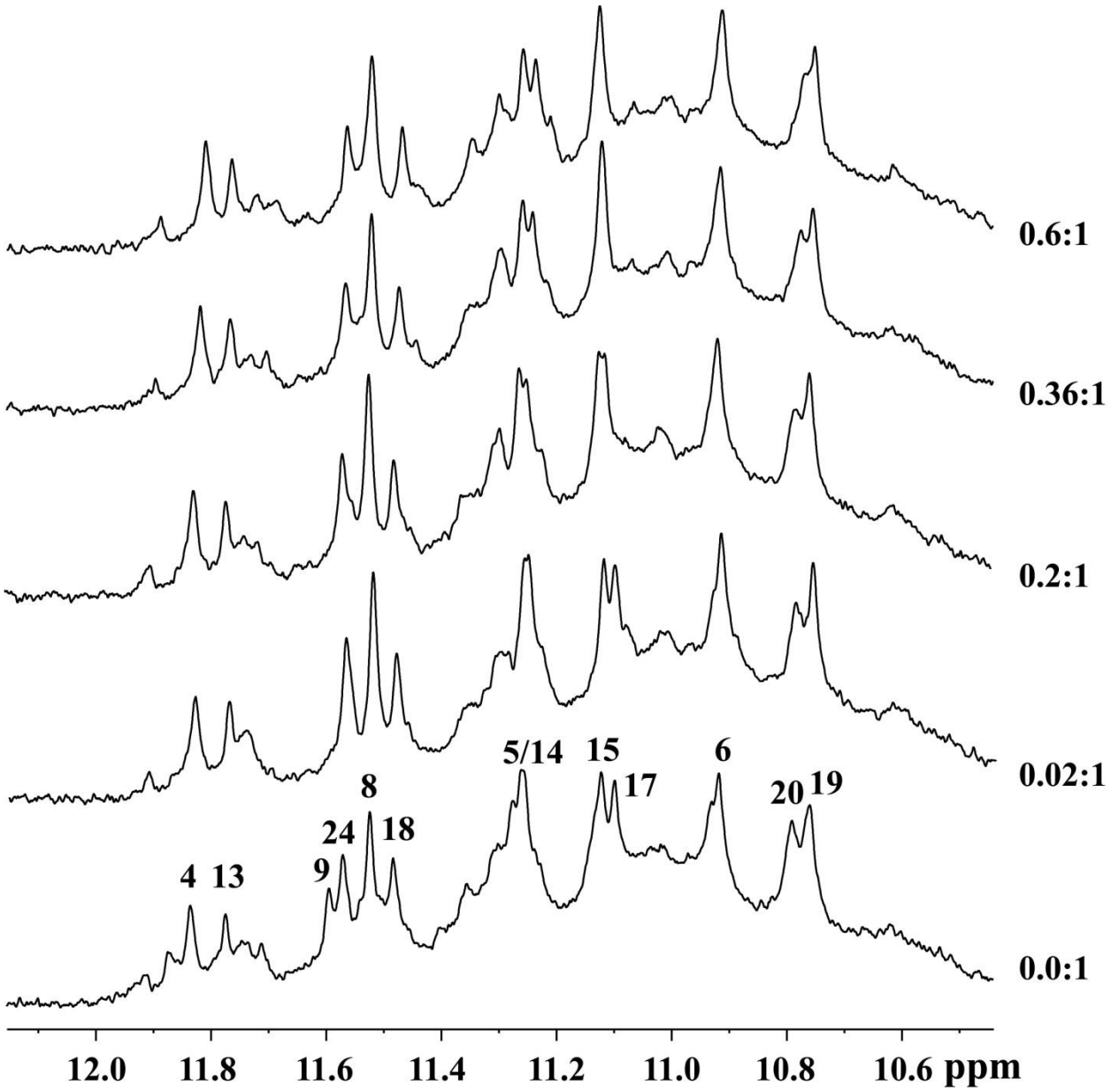

Figure S12: NMR spectra showing the changes in imino region of *Pu24* when titrated with increasing concentration of TPP using one dimensional proton NMR spectroscopy. (Concentration ratio mentioned is for TPP:*Pu24*)

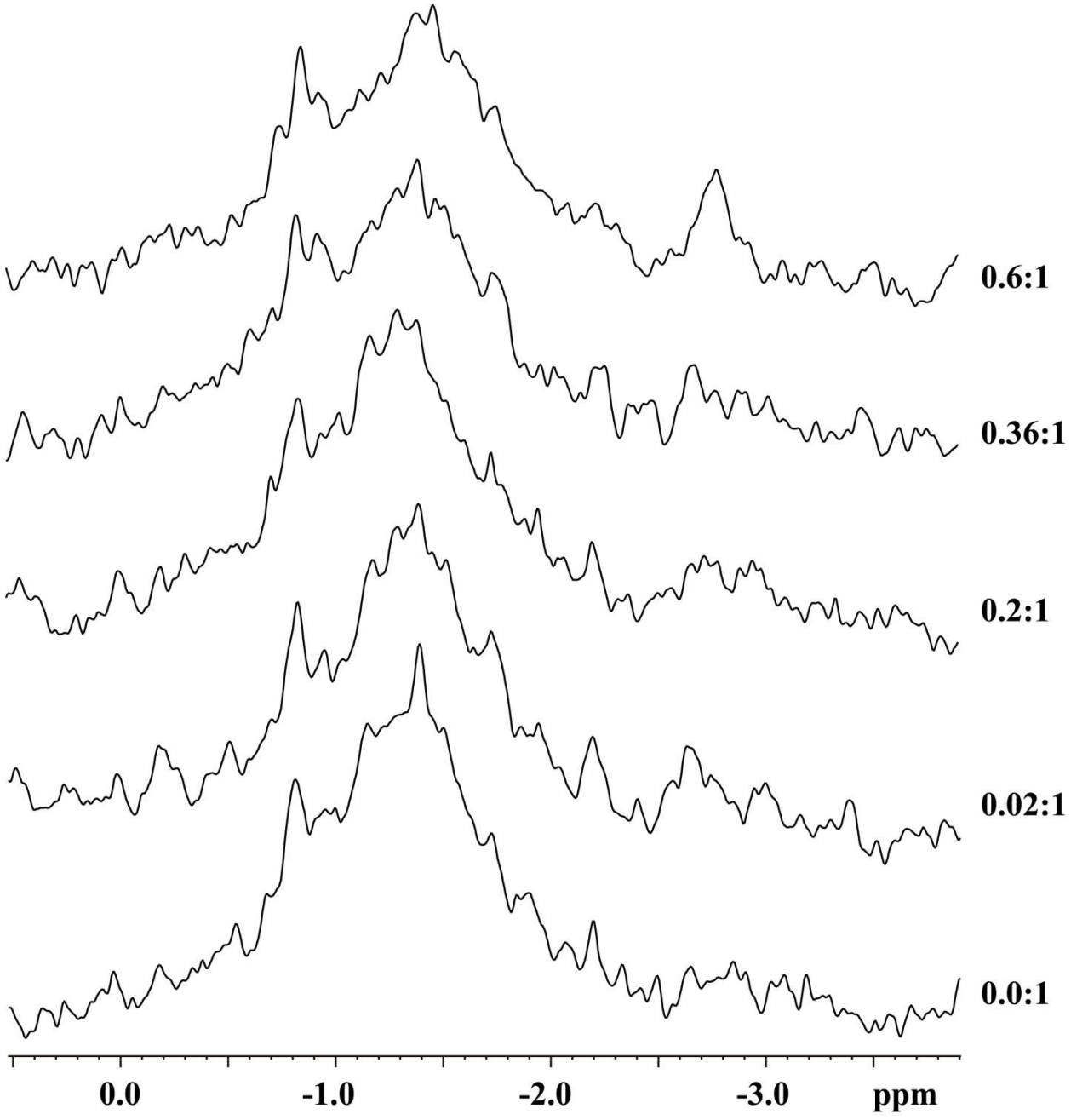

Figure S13: Change in one dimensional ^{31}P NMR spectra of *Pu24* with the increasing concentration of TPP. (Concentration ratio mentioned is for TPP:*Pu24*)

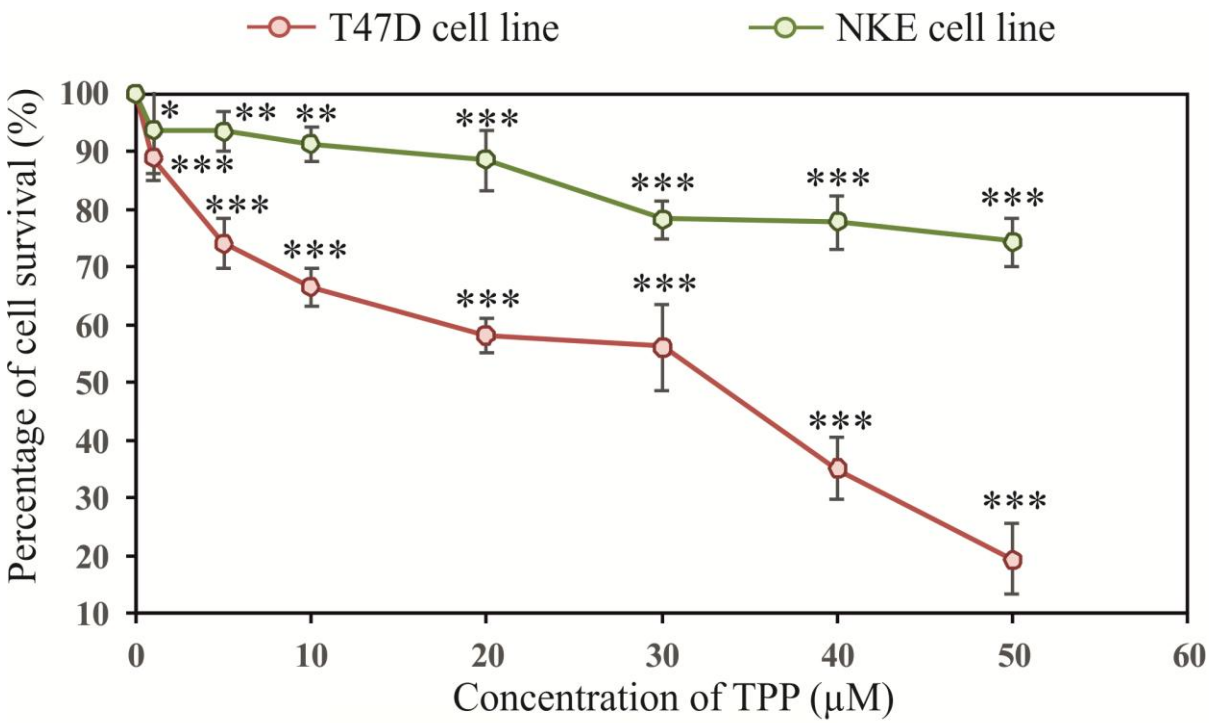

Figure S14: Percentage of survival (%) in T47D and NKE cells at increasing TPP concentration for 24 hours.Error bars in the dot plot represent means ± s.d. from six independent experiments in triplicate. Asterisks (*) indicated statistical significance as determined from Student's t-test compared with that of untreated cells (* indicates P<0.05, ** indicates P<0.01, *** indicates P<0.001).

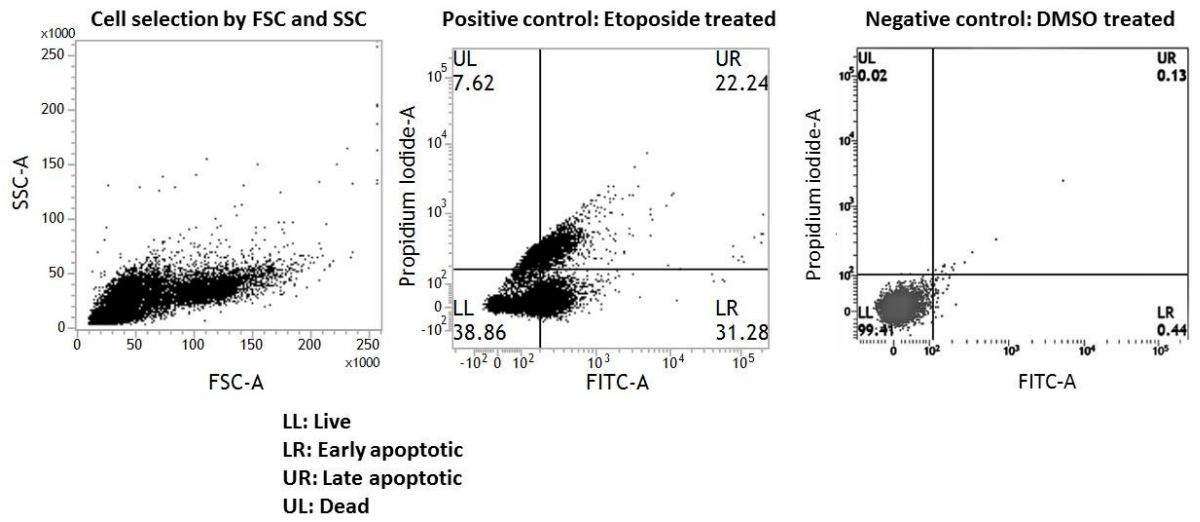

Figure S15: Positive and negative controls of Flow cytometric analysis, (A) T47D breast cancer cells are gated based on the FSC (Forward scatter) and SSC (Side scatter). (B) Positive control for flow cytometric analysis is carried out by treating cells with Etoposide. (C) Negative control is performed using DMSO treated T47D cells as TPP is dissolved into DMSO. LL (Lower left), UL (Upper left), UR (Upper right), and LR (Lower right) in the four quadrants represent Live, dead, or necrotic and early apoptotic stages of the cells upon Etoposide and DMSO treatment.

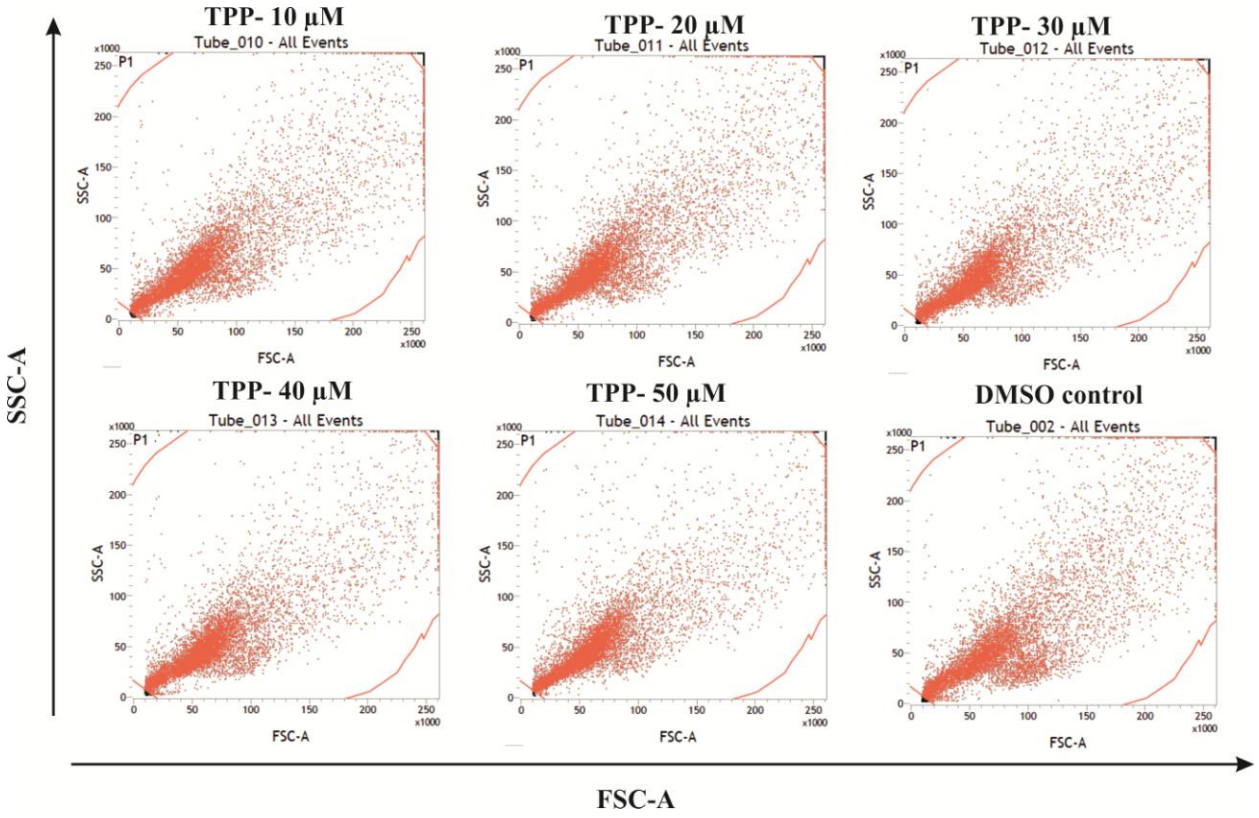

Figure S16: The subset of flow cytometric data has been defined through gating over the SSC vs FSC dot plot for the evaluation of apoptosis and necrotic population. The resulting quadrants of the control and treated sets depict the fluorescence properties of the gated population only.

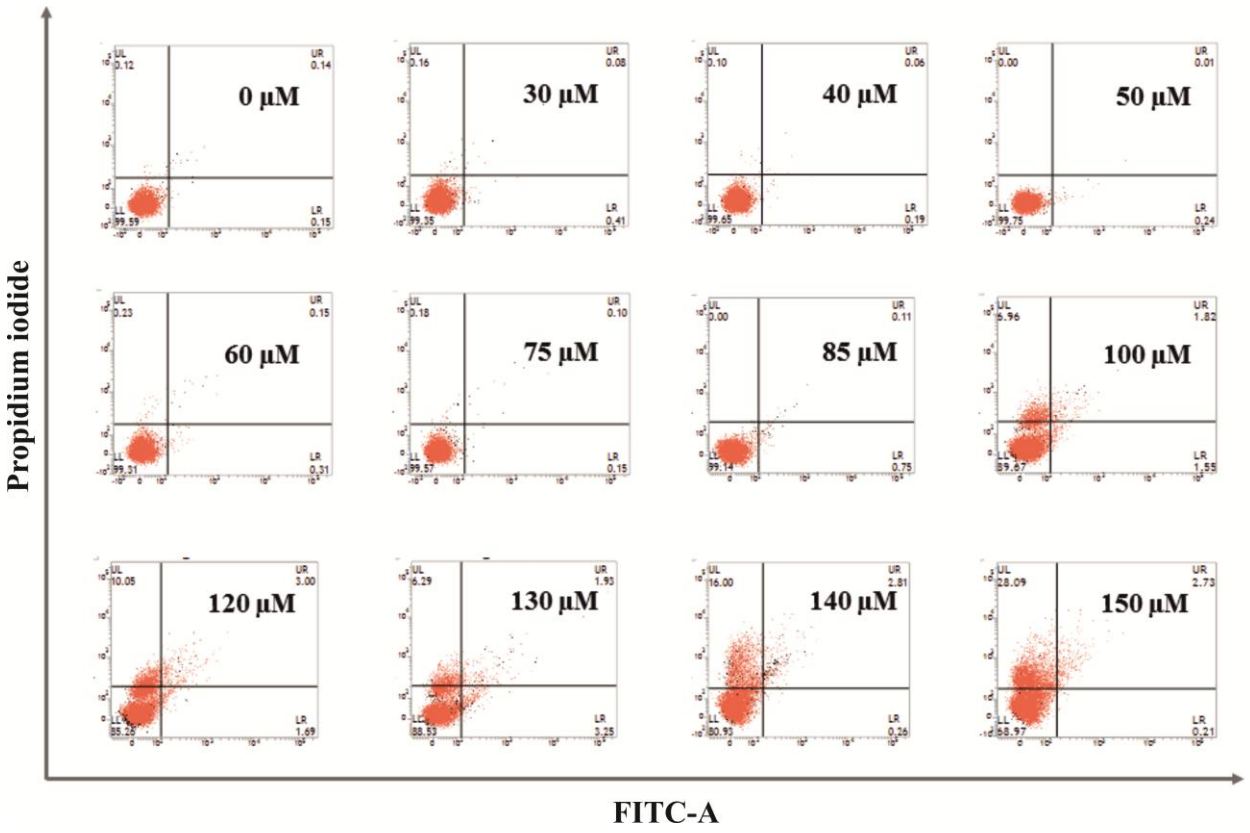

Figure S17: TPP does not exhibit cytotoxic effect upon NKE (normal kidney epithelial) cell line: (a) FACS dot plots showing the apoptosis induction in NKE cell line upon treatment with TPP at increasing concentrations upto150 µM. NKE normal kidney epithelial cells were exemplified from apoptosis induction. A small hike necrotic population is found gradually from 100 µM onwards (6.96%, 10.05%, 6.29%, 16%, and 28.9% at 100, 120, 130, 140 and 150 µM respectively)